Feasibility Study of X-ray Free Electron Lasers in Fourth Generation Storage Rings

Jordis Hansen

A thesis presented for the degree of
Bachelor of Science

LUND
UNIVERSITY

Supervised by:	Francesca Curbis
	Sverker Werin
Project duration:	4 months
Examination date:	01.06.2023

Acknowledgements

I would like to thank Francesca Curbis and Sverker Werin for guiding me through this project, helping me discuss all the questions I had, and all the valuable feedback. I greatly appreciate all the time and care you put into this process. I would also like to thank Johan Lundquist and everyone else at MAX IV who has been incredibly welcoming. Moreover I would like to thank my family for being interested when I talked their ear off about physics, and my friends for all the help and support.

Abstract

This thesis studies the feasibility of a cavity based X-ray free electron laser in a fourth generation storage ring. The cavity design allows for modulation of the electron beam over several passes through the undulator. Simulations based on the PETRA IV facility are done to create the photon flux spectrum of a light pulse produced by an undulator. This spectrum is subsequently modeled to pass through an optical cavity with four diamond mirrors, and the efficiency of the cavity evaluated. A direct comparison to the shotnoise of the beam is made, to determine whether the light after one pass through the cavity will be intense enough to start the amplification needed for coherent emission. The effects of the energy spread and peak current are analysed: decreasing the energy spread and increasing the peak current have both the same effect of increasing the energy of the light produced in a single pass. The central result of the study is that the cavity based X-ray free electron laser seems feasible.

Abbreviations and Acronyms

FEL - Free Electron Laser
XFEL - X-ray Free Electron Laser
CBXFEL - Cavity Based X-ray Free Electron Laser
LINAC - Linear Accelerator
PETRA IV - Positron-Elektron-Tandem-Ring-Anlage
in English: Positron-Electron Tandem-Ring Facility
DESY - Deutsches Elektronen-Synchrotron
in English: German Electron-Synchrotron
SR - Storage Ring
TGU - Transverse Gradient Undulator
VUV - Vacuum Ultra-violet
SIMPLEX - SIMulator & Postprocessor for free electron Laser EXperiments

Contents

1 Introduction

Science relies on experiments to obtain data and better understand the world. In turn these experiments rely on tools, and how science develops these tools. Within synchrotron radiation science, many different types of light sources have been developed and tested, allowing for experiments in fields ranging from material science over medical research to fundamental physics and chemistry. Light sources are upgraded continuously resulting in smaller beam sizes and divergences, that in turn lead to higher brilliance. A consequence of this evolution is the need to study whether schemes previously thought impossible have, with technological advancement, shifted into the realm of possibility. One such question is whether it has become feasible to design X-ray Free Electron Lasers which can be integrated into fourth generation storage rings. These are facilities which have been or will be rebuild based on new and improved design caused by new storage ring technology [1]. They have more favourable properties for optical cavity FELs, such as lower beam emittances, which in turn can now rely on greatly improved X-ray mirrors. Furthermore, undulators have been developed, which may also improve the performance of such a scheme, making this feasibility study relevant to conduct at the current time.

Synchrotron radiation is produced by charged particles that are forced to change the direction of their velocity, most commonly in long periodic arrays of magnets called undulators. The advantages of synchrotron radiation for experimental research are numerous. Fundamentally, it is a reliable way to produce high intensity light pulses with a high degree of control over the light properties. Depending on the production method spectral broadness and pulse length can be picked. Moreover monochromacity, different polarisations and transverse coherence can be achieved and central wavelength chosen. As such synchrotron radiation is used in experiments where bright and short light pulses are needed. Such experiments include testing of material properties, mapping proteins for medical research and life-science applications.

Free Electron Lasers (FELs) are one specific type of machine that can produce fully coherent light. They create light beams by feeding an electron beam through one or several undulators, with the final wavelength depending on both the undulator and beam parameters. Most FELs are used in combination with linear accelerators, as the bunches produced in them have a high enough peak current and low enough emittance to successfully drive an FEL. One such example is the European X-Ray Free-Electron Laser Facility, a 3.4 km long laser in Germany [2]. This length is required as the interaction between the produced radiation and the beam needs time to reach coherence, thus a long undulator is needed. In order to implement FELs in storage rings, which only have short straight sections on the order of meters or tens of meters, it is necessary to add an optical cavity to the set up, as illustrated in Figure 1. By recombining the light, once it has been guided through the cavity, with a new electron bunch from the storage ring, the light is amplified

each trip through the cavity until the laser reaches saturation. These optical cavity based FELs have been successfully used in storage rings down to the vacuum ultraviolet (VUV) wavelength range [3].

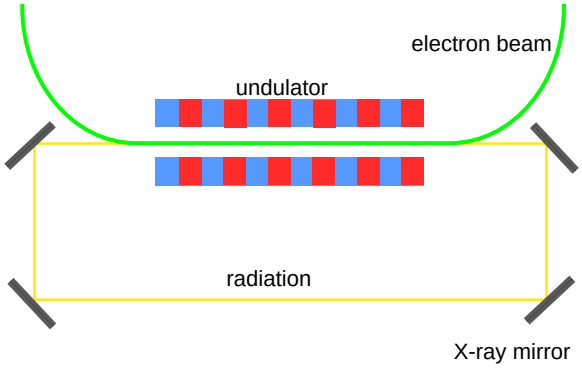

Figure 1: A sketch of the cavity X-ray FEL set up, including the electron beam, undulator and mirrors.

This feasibility study will investigate whether it is possible to adapt the parameters of an optical cavity based FEL to achieve X-ray radiation in fourth generation storage rings. These upgraded storage rings have smaller transverse beam sizes and divergences, which is favourable for storage ring FELs, and moderate peak currents. The MAX IV storage rings in Lund, Sweden have already been updated and are currently in use [4]. Another facility hoping to upgrade their technical designs to fourth generation standards soon is the PETRA ring in Hamburg, Germany [5]. Both facilities would be possible candidates for a storage ring FEL operating in the X-ray wavelength range. One significant challenge with the implementation of storage ring FELs is the relatively large energy spread of the bunches in the ring. To determine their feasibility one has to combine realistic beam parameters and undulator parameters needed for X-ray light emission. If the initial combination of parameters does not result in favourable light properties, other possible technologies must be tested to thoroughly study the options for a storage ring FEL.

Storage ring FELs utilise cavities in which mirrors feed the light emitted back into the undulator. What separates X-ray cavities from UV cavities are hence the mirrors, which need to be reflective in a different wavelength region. Most materials have a very low reflectivity in the X-ray range and additionally the reflectivity is highly dependant on grazing angle and material impurities. Hence, X-ray mirrors were a big challenge and part of what impeded the successful implementation of X-ray free electron lasers (XFELs) in storage rings. However, there have been great improvements in the area of X-ray optics, with diamond and silicon mirrors both being successfully characterised for X-ray optics [6][7]. These mirrors have a reflectivity of more than 99 % in the X-ray region, but they have very narrow bandwidths. Hence the focus will be on testing whether PETRA IV gives rise to parameter combinations compensating for this narrow bandwidth, or pointing out

which parameters prevent successful implementation of an X-ray FEL.

The appeal of building storage ring FELs is the naturally high repetition rate, on the order of MHz of the bunches, along with storage rings serving many beamlines simultaneously. Another advantage of FELs over spontaneous undulator radiation is that they reach a much higher brightness at saturation. As the optical cavity allows for increasing the total radiation with each pass, the FEL can reach saturation even with its limited size. In comparison, the brightness of undulators is still several orders of magnitude lower than the one of FELs [8]. For the experiments the main appeal of FELs over undulators is the coherence of the light. Unlike synchrotron radiation, FELs produce transversely and (with seeding longitudinally) coherent light, which is of great interest to the kinds of experiments conducted at storage ring facilities. Transversely coherent light disperses less when interacting inside a medium [9]. This reduction of dispersion decreases loss of information in the experiment. As many experimental groups rely on diffraction methods and other forms of imaging this would improve experimental results, and allow for the measurements on smaller scales.

Combining all of these consequences of the storage ring XFEL shows that it would change and improve the way X-ray radiation is produced at storage ring facilities such as PETRA IV. Conducting a feasibility study is the first step to finding out which parameters of the electron beam are most decisive as well as what technical aspects may be impossible today. Incorporating an XFEL design into storage rings would equip them with a transversely coherent, bright X-ray laser. This would open the opportunity for a wider range of experiments at these facilities.

2 Theory

2.1 Synchrotron radiation

The concept of electromagnetic waves being emitted by an accelerated or deccelerated electric charge already became apparent from Maxwell's equations in 1873. Still it was not until more than twenty years later that Larmor derived an expression for the power radiated by the acceleration of a charged particle and Liénard extended this to the radiation of relativistic particles along a circular path. The energy lost by an accelerated charged particle became truly relevant when particle accelerators were being constructed, as synchrotron radiation causes an energy loss and thus limit the maximum energy. Synchrotron radiation also affects the beam dynamics through radiation dampening of the energy and it in turn affects the beam dimension and magnitude. Furthermore, it affects the mechanical components of the accelerator, as the radiation can cause the release of small particles inside the vacuum. In the early days of accelerators and storage rings, the main application was high energy physics. Synchrotron radiation was hence mostly a complicating effect. However the potential of synchrotron radiation as tool was soon recognised, and facilities were being built specifically to produce light through this mechanism. The first facilities built specifically for this were the SURF and INS-SOR rings in 1963. What made synchrotron radiation attractive as light source was the ability to produce high intensity photons beams that were small in size and polarised [10].

Synchrotron radiation is also called magneto-bremsstrahlung, and is exhibited by all charged particles being accelerated or decelerated. It is emitted during both linear and circular motion, but the emission increases with a factor of γ^2 under circular motion, where γ is the Lorentz factor of relativistic motion defined as

$$\gamma = \frac{1}{\sqrt{1 - \frac{v^2}{c^2}}} \, .$$

For circular motion the radiation power, as given by Larmor, is proportional to γ^4. Since the Lorentz factor is proportional to the total particle energy, through $\gamma = \frac{E}{m_0 c^2}$, light particles will radiate significantly more than heavy particles of equal energy E. That is why synchrotron radiation facilities usually use electron beams to produce a higher photon flux, as they are the lightest charged particle. Synchrotron radiation itself is emitted in all directions, but as the electrons are relativistic the radiation is boosted in the direction of motion of the bunch. Therefore, the light pulses created only have a small angular divergence which is favourable for many experiments [11].

2.2 Producing Synchrotron Radiation

Synchrotron radiation is produced via different types of magnetic structures, which yield different spectral and intensity properties. The simplest way to produce synchrotron radiation is using a bending magnet, with no further interaction beyond the radiation of photons. The pulse emitted is short in time and exhibits a broad wavelength spectrum. But as synchrotron radiation science developed, so did insertion devices, which are inserted into the straight sections of storage rings. They usually are a series of magnets moving the beam along a sinusoidal path to create more photons. Depending on the specific magnetic field structures of these insertion devices, they can achieve higher photon energies, higher photon flux, increased brightness and different polarisation and coherence properties [11].

Differently to a single bending magnet, most insertion devices provide a periodic magnetic field. Depending on what the insertion devices are optimised for, they may be further sub-categorised. One of the main insertion devices are undulators, which cause small undulations leading to a single light pulse with a narrow bandwidth.

The structure of the undulator is periodic, with the length of one period being the undulator wavelength λ_u. Electron bunches accelerated along the sinusoidal path caused by undulators will then predominantly emit at λ_u. However as the electron bunch is moving at relativistic speeds, in its coordinate system it will view the undulator period contracted. In turn the radiation that will then be emitted is, as seen in the lab frame, further Lorentz contracted so that the emitted light will then have the wavelength $\lambda_r \approx \frac{\lambda_u}{\gamma^2}$ [12]. Furthermore the Lorentz boost in the electron beam direction causes the light to be emitted in a narrow cone, with the maximum angle at which light is emitted being θ_{max}. The undulator parameter K is defined as

$$K = \frac{eB\lambda_u}{2\pi m_e c} \ ,$$

where B is the peak magnetic field of an undulator, but can also be estimated from the cone of emission through $K \approx \gamma\theta_{max}$. The expression for the resonant wavelength of the light is then

$$\lambda_r = \frac{\lambda_u}{2\gamma^2}\left(1 + \frac{K^2}{2}\right) \ .$$

2.3 Free Electron Lasers

What distinguishes free electron lasers (FELs) is their potential to produce fully coherent bright light. They utilise interaction between radiation and electrons to achieve coherence. As the bunch moves through the periodic field of the undulator, it interacts with the light

it has already emitted. This interaction leads to Self Amplified Spontaneous Emission (SASE) where the previously emitted light acts as seed for monochromatic photon emissions. Furthermore, this interaction between light and electron bunch causes electrons to organise themselves into regions smaller than the radiation wavelength to radiate as one "macro-particle". The distance between the modulated regions is exactly one wavelength λ_r resulting in coherent radiation. Additionally, coherent emission increases the intensity, I, as incoherent emission intensity scales as $I \propto N$ while coherent emission intensity scales as $I \propto N^2$, where N is the number of electrons in a bunch. Hence FELs produce near monochromatic and coherent light pulses, if given enough space for the interaction between electron bunch and light.

Inside the undulator the radiated light forms an electric field which interacts with the electron beam itself. The individual electrons move transversely in the undulator and depending on the respective orientation between transverse motion of the electrons and the electric field of the light, energy can be transferred from the wave to the particle or vice-versa. Therefore, the electrons can either gain or lose energy, as shown in Figure 2. The resulting change in velocities leads to the formation of smaller structures inside the electron bunch, which is also called beam modulation. As modulation is caused by the undulator radiation, the modulation has the periodicity of one radiation wavelength λ_r and the electrons will now emit fully coherent light as they move through the undulator. In Figure 2, there is no net energy transferred between electrons and light. As they continue to move with respect to each other, the electrons will be slowed down by the radiation. The change in kinetic energy is then transferred to the radiation, further amplifying the radiation power.

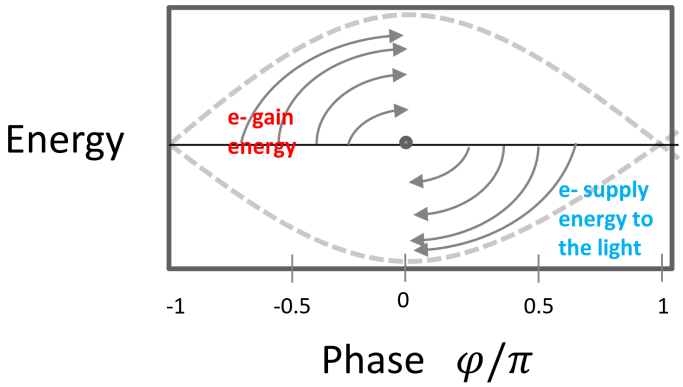

Figure 2: Sketch of the energy transmission between radiation and electron bunch resulting in modulation of the bunch. Figure taken from [13] with permission from author.

Typical FEL design will often feature long undulators to ensure the transition from spontaneous emission to coherent emission, but the design can be adapted through the use of a cavity, as will be explained in section **2.5**, to rely on a much shorter undulator.

2.4 Shot Noise

Within the electron bunch entering the undulator, the electrons will be somewhat unevenly distributed. This leads to some microscopic structuring of the beam, which in turn will cause different wavelengths to be emitted with higher intensity than others. As this is a random distribution the spectrum is broadband with no discernible structure. This effect competes with the structuring/bunch modulation caused by the seed light. As the effect is caused by random shot-to-shot fluctuations within the bunch, it is called shot noise.

In FEL simulations there is an additional numerical shot noise introduced by simulations. As simulating every single electron is very computationally intensive, simulation programs group electrons with similar positions in phase space together into beamlets. Instead of simulating the behaviour of individual electrons, the beamlets with a larger charge are then used as macroparticles in the simulation. However this also introduces an artificial structuring in the bunch which will lead to additional shot noise in the simulation. The relevant effects for this study are further explained in section **3.2**.

2.5 Cavity based design

There is a variety of different cavity designs for cavity based XFELs, which have different specific advantages. The fundamental concept however remains the same: radiation from a single pass through an undulator is stored in the cavity and fed back into the undulator timed to match the arrival of the next electron bunch. As the single pass spectrum is much broader than the bandwidth of the mirrors in the cavity, the cavity selects the specific photon energy which will be amplified. In addition to at least two mirrors cavities also use grazing incidence mirrors to control the light beam properties. A two mirror set up can be seen in Figure 3. The length of the cavity, L, is typically much larger than the undulator, i.e. on the order of around 100 m, while the cavity can be kept very narrow. The exact length of L is determined by matching the cavity round-trip time of the light to the electron bunch frequency in the ring [14]. In order to use the FEL light for experiments, one of the mirrors will typically let around $4 - 5\,\%$ of the light through. If the FEL gain overcomes the cavity losses, the pulse energy will increase exponentially until it reaches saturation.

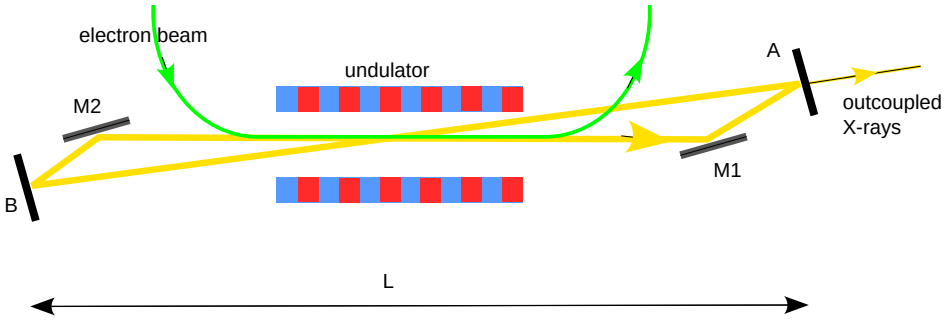

Figure 3: Schematic of a two mirror cavity. The diamond crystal mirrors are denoted A and B while the grazing incidence mirrors are denoted M1 and M2.

X-ray cavities require mirrors with reflectivity in the X-ray range that can handle the heat load of the light pulse and cause minimal wave-front distortion to the light pulse. X-ray mirrors use Bragg reflection of lattice planes in crystal structures. The ideal candidates for X-ray mirrors are elements with a low atomic number, as they form crystals with close to perfect reflectivity with only a few lattice planes needed. Amongst the attractive crystals are for example Diamonds, Be, and SiC. Diamond is particularly of interest, due to it having high thermal conductivity, low thermal expansion and the ability to produce it with few impurities [14]. Another popular candidate is silicon, as pure silicon mirrors also exhibit excellent X-ray diffraction properties. Both carbon and silicon diamonds have been tested both in terms of reflectivity and thermal responses, and have been deemed feasible for X-ray cavities [6][14].

The simplest cavity design uses only two mirrors, however this set up is not tunable. By increasing the number of mirrors to a minimum of four it is possible to achieve a large tuning range. This gives the setup a lot more flexibility to experiments, however, the addition of mirrors sets higher requirements on the FEL as the cavity will be less optically efficient. By expanding the cavity to four mirrors as shown in Figure 4, the cavity becomes tunable to a large range of energies. This works by changing the angle of incidence on all four crystals. In this set up the positions of mirrors A and D are fixed, and in turn so is L. Then by changing the positions of mirrors B and C, the incidence angles of all four crystals can be controlled, while maintaining the timing necessary for meeting the next bunch in the cavity. The change in photon energy changes with the incidence angles as the Bragg energy is dependent on the incident angle. Changing the mirror position in a multi mirror cavity by up to 1 m can change the photon energy by around 1 keV, assuming an average energy of ≈ 15 keV. It is possible to design multi-user cavities using more mirrors as well, where several crystals outcouple parts of the radiation [14].

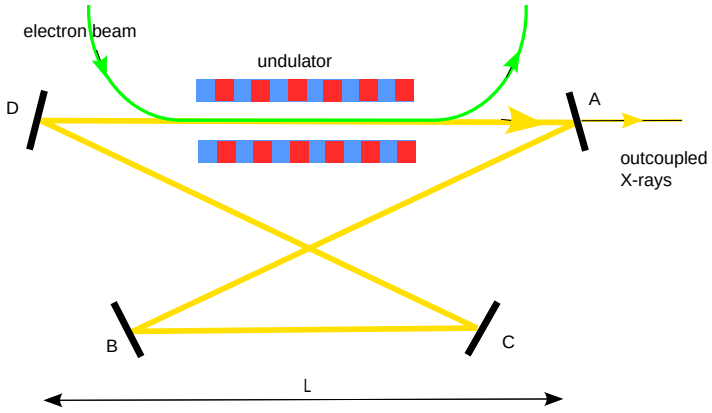

Figure 4: Schematic of a four mirror cavity. The diamond cystal mirrors are denoted A, B, C and D.

Full X-ray cavities are currently being tested in several facilities. One such cavity consisting of four diamond mirrors was tested for round-trip efficiency by coupling a femto-second FEL pulse into it at the SLAC National Accelerator Laboratory, California, USA. The study show that light can be trapped in the cavity in a stable mode, providing strong support for the feasibility of a cavity based XFEL [15]. Another proof-of-concept cavity which is expected to yield results in 2024 is being constructed at the European XFEL. This cavity will also feature four diamond crystal mirrors which will be cryogenically cooled [16].

2.6 Storage Rings

Storage rings can be classified into different generations based on their intended uses and light produced. The first storage rings were constructed for high energy physics and only used parasitically as light sources. This proved so useful that synchrotron radiation programs were started and the second generation of storage rings were constructed. As insertion devices were still being developed, these rings had many bending magnets to be used as light sources.

The third generation of storage rings brought around two major changes. They had many straight sections for the use of insertion devices and focused largely on reducing the beam emittance, as it has a large effect on the brightness of undulator radiation. The emittance is the product of the transverse size of the beam as well as its divergence. It depends on several factors of the beam design including the electron energy. The designs for the third generation rings achieved emittance of $5 - 20$ nm-rad compared to the hundred to several hundred in second generation ring. This improved undulator radiation brightness from up to 10^{16} photons/(s mm^2 mrad^2 0.1% bandwidth) in the second generation to as high as 10^{20} in the third [17].

The fourth generation of storage rings are presently being built, with some facilities, such as MAX IV finished and already in operation, and other supposedly starting construction soon. The distinction between third and fourth generation is based in performance, with fourth generation rings increasing performance of third generations by at least one order of magnitude within either brightness, coherence or pulse duration. This is possible as third generation rings are still far from fundamental limits of the produced radiation. The goal of these new facilities is to offer brighter and more coherent light, especially within the very ultra violet and X-ray regions.

2.7 PETRA IV

PETRA IV (Positron-Electron Tandem Ring Accelerator IV) will be the upgrade of the current PETRA III storage ring and synchrotron radiation source at DESY (Deutsches Elektronen-Synchrotron) in Hamburg, Germany. As such it will be built into the already existing tunnels, and the geometric properties remain the same as in PETRA III. Similarly the electron beam energy will remain at 6 GeV. The changes will occur within the magnetic structures in order to optimise the other beam qualities for light production. The conceptual design for the upgrade is complete and has been published in the Conceptual Design Report in 2019, wherein the specific properties predicted for the facility are listed and described [18]. The final design report is expected to be published within months of the publication of this study, and the PETRA IV storage ring is planned to enter operation in 2027.

The PETRA tunnel has a circumference of 2304 meters and is among the biggest storage rings in the world. This in turn means that the straight sections within the ring are comparatively long as well. The PETRA tunnel has two types of straight sections: 4 that are 108 meters long and 4 that are 64.8 meters long. This study focuses on the shorter straight sections, as a team at DESY has used these for a similar study about an optical solution providing constant focusing in the undulator. In the study they conclude that it is feasible to have a 30 meter undulator within the straight section [19]. The undulator can not take up the entire straight section as focusing elements correcting and optimising the bunch entering into the undulator will also have to be incorporated. Hence 30 meters is on the conservative side for the length of the undulator, and should leave significant enough space for the other elements.

3 Method

3.1 Choice of set-up

As a basis for the simulations electron beam parameters and undulator set up was selected. As the set up is based on the planned PETRA IV ring, the beam parameters that form the basis of the study are taken from the conceptual design report [18] as well as [5] as listed in Table 1.

Beam parameter	Unit	Value	Source
Electron energy	GeV	6	[18], [5]
Bunch length	m	199e-4	[18]
Bunch charge	nC	7.69	[18]
e_x	mm mrad	0.187	[18]
e_y	mm mrad	0.0374	[18]
Energy spread		0.73e-3	[5]

Table 1: The original beam parameters of PETRA IV, used as the basis for the study.

The next essential part of the set up is the undulator. For this the length, focusing, undulator parameter etc. had to be decided. As described in the theory section a previous study had found that the straight sections in the PETRA III tunnels could support a 30 m long undulator. For this study the undulator was modelled as one segment such that the focusing was optimised through the entire undulator without the need for further optics in between undulator segments. As such the length of 30 m can house 1500 undulator periods of 2 cm each. Combining this with a undulator parameter $K = 0.793$ centres the FEL radiation at a wavelength of 0.9534 Å. This specific radiation wavelength was chosen as it corresponds to one of the allowed Bragg energies for a diamond crystal.

For the modelling of the cavity, the focus was not on the geometric set up itself, but rather on the effect on the spectral intensity of the radiation. The reflectivity of the mirrors was the component of the cavity incorporated into the analysis. For the cavity, diamond mirrors were chosen, as there are calculations done on the bandwidth for numerous different lattice planes of pure diamonds, as well as the advantages of diamond mentioned in section **2.5**. For this study the $hkl = 642$ lattice plane was chosen which has a corresponding Bragg energy of 13.0051 keV [20]. This particular lattice plane has a bandwidth of 21.3 meV. In general, for diamond mirrors the bandwidths for reflectivity on the X-ray region is between $5 - 24$ meV. Within this region the reflectivity was then modelled as 99 %, as previous studies of diamond mirrors have shown a reflectivity of more than 99 % within the region of reflectivity [14].

As the simplest tunable cavity design requires four mirrors, the spectrum produced by a single pass was modelled to be affected by four mirrors, three of which having the men-

tioned reflectivity, and one having an additional four percent of light outcoupled. The outcoupled light is what will be used in experiments.

3.2 Simulations

For the simulations done to conduct this study the program SIMPLEX (SIMulator & Postprocessor for free electron Laser EXperiments) was used [21]. The beam input was based on the parameters shown in Table 1 and only changed when scanning individual beam parameters. As for the undulator, the properties are described above, and it was modelled as one segment with optimised beta functions throughout the undulator. A lot of the work was done to ensure that the simulations were done consistently and reliably and to eliminate errors originating from the set up of simulations.

Simulating FEL radiation from an electron bunch is computationally intensive and only a finite number of particles can be simulated. In order to get as accurate results as possible different approximations can be made in the simulation. SIMPLEX groups electrons with similar properties together into macroparticles, thus decreasing the number of particles to simulate. This is done in slices along the bunch. The slices are needed in order to account for slippage effects between the radiation and the electron bunch. In time dependent mode, simulations are done slice by slice which allows for different amount of interaction between electrons in the slice and radiation depending on the radiation strength and peak current at that position. For this study a maximum of four macroparticles per beamlet, as mentioned in section **2.4**, and eight beamlets per slice were used.

Furthermore, as not every electron is simulated individually along the bunch, different simulation controls are needed for accurate results for radiation power and spectrum. To simulate the power of the light pulse a bigger section of the bunch, in this case the central 10 %, was simulated. However, to have a better resolution in the radiation spectrum only the central part, specifically the central 0.1 % of the bunch was used with a small step between the slices.

SIMPLEX is not capable of modelling a precise shot noise spectrum as it uses beamlets, which introduces numerical shot noise as mentioned in section **2.4**. However, it calculates the peak power of the shot noise in order to implement shot noise seeding depending on beam parameters. SIMPLEX then has the function of implementing an artificial seed which is a narrow peak centred around the undulator radiation wavelength.

In order to simulate the shot noise spectrum a combination of the peak power, calculated for the undulator set up, and the seed function was used. To utilise the seeding function in SIMPLEX only two undulator periods were modelled yielding virtually no interaction of the beam and undulator. This resulted in a spectrum consisting of only the

shot noise seed. The power estimated by SIMPLEX for the FELs shotnoise was compared to the seed simulations, to ensure they had the same intensity.

The actual shot noise spectrum is be the result of random emissions, and will result in a broad spectrum. However, the seed function gives only a narrow peak in the wavelength spectrum, representing a single narrow window of the broad shotnoise spectrum. The peak value is then used as a maximum value within the narrow bandwidth, so that the shotnoise is approximated as constant. The python code for this analysis is listed in the Appendix.

4 Results and Discussion

4.1 Combining FEL and shot noise spectra

The spectrum of the light pulse produced by a single pass of the undulator is shown in Figure 5. The total photon flux shows the number of photons in the light pulse per photon energy bin. It is centered around a wavelength of 0.953 Å. The implementation of the cavity resulted in the second spectrum shown in Figure 5, showing the remaining photons after one pass through the four mirrors. This illustrates the difference in broadness between the undulator spectrum and the narrow bandwidth of the diamond crystals. While the reflectivity even after four mirrors and an outcoupling of four percent of the radiation is very high, the vast majority of synchrotron radiation produced in the first undulator pass is discarded through heat load in the crystal. This is why a fast amplification of undulator radiation within the desired bandwidth is desirable.

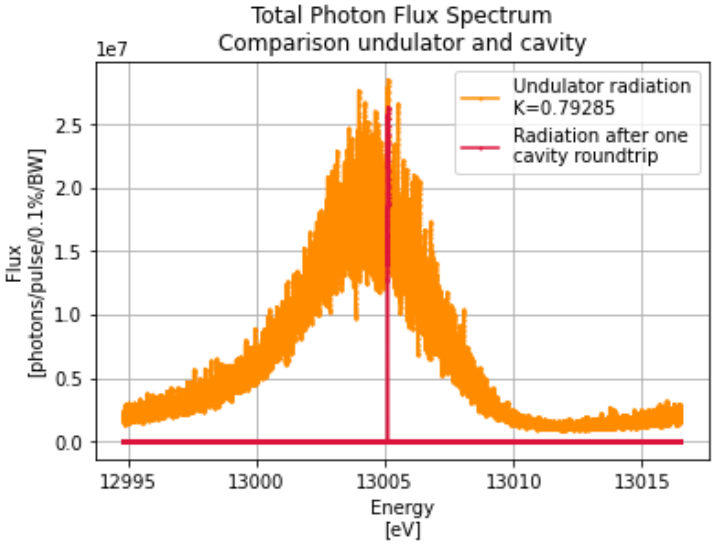

Figure 5: The total photon flux for the undulator spectrum along with the light surviving the cavity.

As the cavity is modelled with a high efficiency, the losses are very low and the intensity of the light depends mostly on the tuning between cavity and undulator. Due to the very narrow crystal bandwidth, the selection of wavelength will greatly affect the photon flux. To analyse what happens when the undulator spectrum peaks outside of the cavity bandwidth, the undulator was tuned less accurately to the cavity by changing the undulator parameter K from 0.7928 to 0.793. The resulting spectrum is shown in Figure 6. Here the flux remaining after the cavity is lower than in Figure 4, as the cavity selects a different portion of the spectrum. As shown the same reflectivity yields here only half of the photon flux, which will make the cavity much more sensitive to the shot noise, which is much broader than the spectrum.

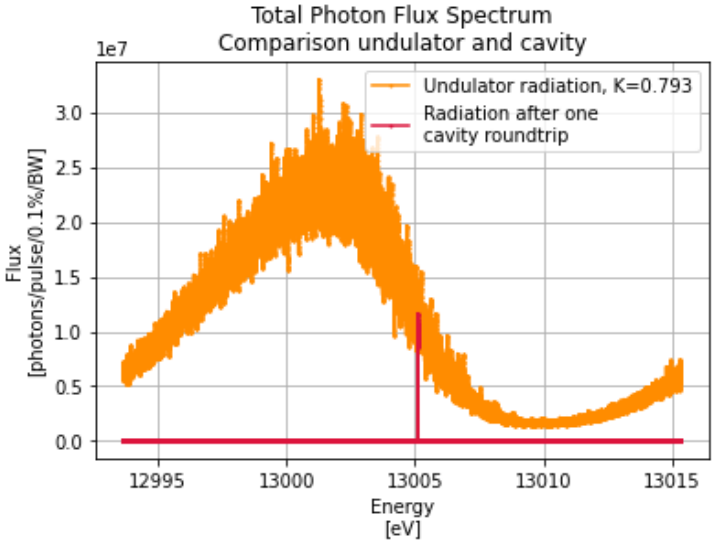

Figure 6: The total photon flux for the detuned undulator spectrum along with the light surviving the cavity.

The first comparison needed to make an evaluation of the XFEL cavity feasibility is between the light surviving the cavity and the shot noise of the beam. In Figure 7 this is done by modelling the cavity as four mirrors as described in section 2.1 and as having no other losses. It can be seen that the light after one pass through the cavity is greater than the shot noise by about a factor of 2. This is a very positive result for the feasibility of a cavity based XFEL (CBXFEL), as the remaining light would induce modulation in the subsequent electron bunch leading to an amplified emission within the bandwidth. When looking at the case with a detuned undulator, the flux remains above the maximum shot noise level, however it has a much smaller margin. In this case any additional cavity losses that have not been accounted for here will be relevant.

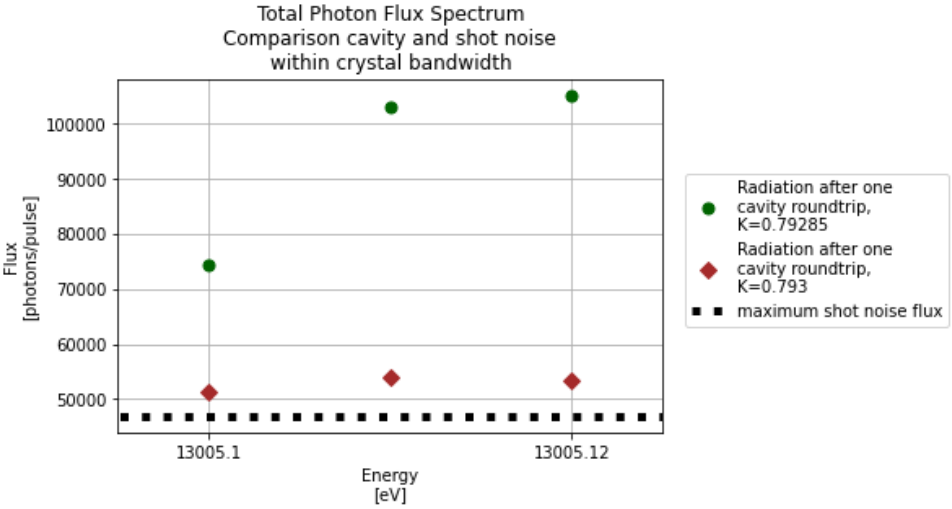

Figure 7: A comparison between the shot-noise and the total photon flux spectra of the two undulator cases.

However multiplying the reflectivity of four mirrors is a highly idealised model neglecting other losses as well as assuming near perfect reflectivity of 99 % in the entire bandwidth. Realistically one has to account for impurities in the crystal, as well as other important losses in the cavity. These could for example be caused by the impact of heat load on the crystals, as the entire part of the spectrum outside of the bandwidth will be absorbed in the first mirror. In these simulations this corresponds to 99.09 of the energy contained in the initial light pulse. Furthermore, the real beam and pulse could have sub-ideal focusing due to shot-to-shot fluctuations or misalignment. Additionally, if the light is not emitted perfectly in line with the mirrors, a further fraction may not intersect with the electron beam, and thus not contribute to the pulse.
In addition to making a direct comparison between light spectrum and shot noise in Figure 7, it is alternatively possible to identify the minimum/threshold cavity efficiency to retain information from the initial pass through the undulator to the next. For the chosen cavity with four mirrors, the maximum acceptable losses within the cavity to maintain flux above the shot noise would be 55.57 %. In the detuned case this drops down to 13.38 %.

4.2 Energy Spread

While the comparison with the shot noise indicates feasibility, it is still beneficial to explore which beam parameters the set up is most sensitive to and which can be controlled in order to improve performance. One aspect of the electron beam properties that has a large impact on the power gained through one pass of the undulator is the energy spread of the beam. The energy spread of the beam arises as not every electron will have the exact same energy, and is caused by variations in each individual bunch. In order to increase the efficiency of a CBXFEL it may therefore be interesting to quantify the exact effect energy spread has on the single pass pulse energy.

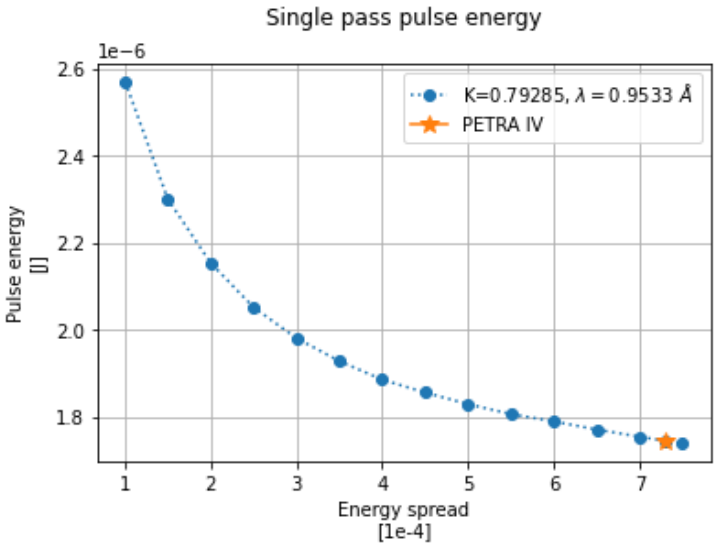

Figure 8: The pulse energies after a single pass through the undulator as a scan of energy spread.

Shown in Figure 8 is the single pass pulse energy from simulations varying only the energy spread and maintaining all other beam parameters from PETRA IV. For comparison the expected energy spread at PETRA IV is 7.3 $\times 10^{-4}$. It can be seen that the pulse energy increases non-linearly with decreased energy spread. As energy spread reduces, a higher fraction of the electrons is close enough to the FEL resonance to contribute to the amplification of the pules intensity, thus increasing the pulse energy.

Another aspect making the energy spread relevant is the ability to modify its effect in the set up through transverse gradient undulators (TGUs) [22]. TGUs minimise the effect of the energy spread by using skew undulators, which results in different field strengths transversely in the undulator. Electrons of different energies then experience different magnetic field strengths, bridging the gap between undulator resonance and electron energy. This results in increased emission, as more of the electrons will be close enough to the FEL resonance. With current predictions for TGU performance it would be possible to model PETRA IV as having an equivalent energy spread of 2 $\times 10^{-4}$. In the results this corresponds to an increase in pulse energy of 18.27 %.

4.3 Peak Current

The peak current in the electron bunch has a large impact on the total pulse energy produced in the FEL. It can be influenced in two main ways, either by increasing the total bunch charge or decreasing the bunch length. Both of these would depend on changing the operational mode run at PETRA IV, of which currently two are planned [18], but are possible within limits. The main challenge arising from increasing the peak current is bunch instabilities.

PETRA IV's conceptual design report [18] anticipates two modes of operation at PETRA IV: one called Brightness and a second called Timing. The brightness mode uses 1600 bunches with a bunch population of 6×10^9 electrons, while the Timing mode uses 80 bunches with 4.8×10^{10} electrons each. The peak current is much higher in the Timing mode with around 46.2 A in peak current, and has been used for this study. The first data point in Figure 9 is based on the unchanged PETRA IV parameters.

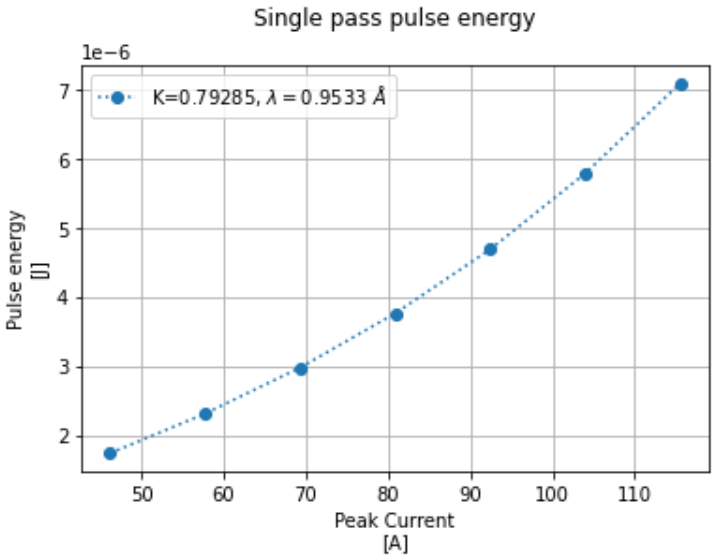

Figure 9: The pulse energies after a single pass through the undulator as a scan of peak current.

As is shown in Figure 9 increasing the peak current non-linearly affects the pulse energy. Any increase in pulse energy after a single pulse will also result in an increased beam modulation for the second pass. Therefore, it will contribute to the radiation reaching saturation quicker. Additionally the energy/power of the final laser pulses will be higher.

4.4 Feasibility

According to this study, a CBXFEL based on the PETRA IV beam is feasible. The light produced after one cavity round trip is enough to cause amplification, as it is brighter than the shot noise inherent to the beam. The performance of a CBXFEL in storage rings would increase with a decrease of energy spread or increase in peak current. A suggestion for an equivalent decrease in energy spread using transverse gradient undulators is made, along with the likely result of such technology.

As lower threshold for feasibility at PETRA IV a cavity efficiency of 15 % was found. As theoretically expected cavity efficiencies are on the order of 85 % are foreseen, this is a very positive outlook [23]. Such a low number indicates that CBXFELs may be implemented at facilities with less ideal parameters such as lower beam energies and shorter straight sections as well.

5 Outlook

As this study has found the cavity based XFEL design to be feasible in the case of PETRA IV, more detailed studies would be beneficial to further understand the strengths and limits of this set up. Firstly, a more detailed study of the undulator spectrum as seeding occurs would give further insight into the exact light properties at saturation. Secondly, studying the cavity components in more detail would give more exact knowledge about the limits of the apparatus. Lastly, to make this study more general it would be interesting to study the behaviour of a cavity based XFEL in other facilities than PETRA IV.

5.1 Study of multiple passes

This study has focused on the principle of feasibility, asking whether the light after one pass through the cavity will be intense enough to start the amplification needed for coherent emission. Hence it centered around the single pass through the undulator followed by a study of the cavity. This leaves room for the exact models of how the light pulse evolves through several passes through the cavity. To do so, the radiation re-entering the undulator could be used as seed light for a second pass simulation using a recirculating bunch in the storage rings.. In such a study the calculations of sensitivity to timing jitters could further be analysed and compared to simulations. Furthermore, the exact number of passes through the cavity needed to reach saturation could be found.

By simulating and studying multiple passes a more detailed insight into the development of the light spectrum would be gained. This would not only test our understanding of such a set up but would also show the exact light source properties once the XFEL reaches saturation, such as the exact brightness and time profile of the light pulse. As this light is what the experiments use, this is an important overview to gain. It can then be compared to the needs of experimentalists utilising the fourth generation storage rings as light sources.

5.2 Different Cavities

Another aspect of CBXFELs warranting further study are the different theorised set ups. As mentioned in the theory section there are options with several mirrors in order to increase tunability and the amount of outcoupled lasers. For a more expansive study of feasibility it is important to consider the differences in these set ups and study in detail how this affects the light production. This includes the effect of optical losses other than the mirrors, as well as the effect of tunability. As tuning these cavities involves rotating mirrors it may change the timing or overall reflectivity of the cavity. Such effects have not been examined closely yet.

It would also prove interesting to study whether there is a timing difference induced by a larger range of tunability. Changing the angle of reflection between several of the mirrors in a cavity would change the roundtrip time, as well as the stretching of the light pulse in the cavity. It has been calculated that a 10 fs error in timing is unproblematic [23], however as the complexity in the cavity design increases this factor of timing error could become more significant.

5.3 Other storage rings

All simulations done in this study were done based on the expected beam properties of PETRA IV, as this facility has many advantages, starting from the comparatively long straight sections allowing for a 30 meter long undulator. It would be interesting to investigate the feasibility of a cavity using a much shorter undulator, to see the limits of feasibility for cavity based XFELs. A good candidate to use as basis for such a study would be a storage ring with shorter straight sections and with a flexible bunch profile, to allow for more possible tuning of the electron bunch with respect to the cavity.

The original aim for this work included a study of the MAX IV facility. As the setting up of simulations took longer than originally anticipated, this part of the study was not completed, but is instead left for future projects. The comparison would be interesting, as the dimensions of the ring as well as beam energies are very different. MAX IV has two active storage rings, one with 3 GeV and one with 1.5 GeV beam energies. Additionally, the rings are much smaller and as such might show the constraints for the feasibility of cavity based storage ring XFELs. Furthermore, the bunches are much longer than in PETRA IV due to the different radiofrequency system used.

5.4 Compatibility of CBXFEL and SR's

The effect on the electron beam of the implementation of CBXFELS has yet to be evaluated. The first passes through the undulator do not alter the bunch much. However, when the amplification of the light occurs, it will affect the electron bunches more significantly. This would impact the other experiments, which makes it an important consideration. How much the ring can accept without affecting the normal operation of other beamlines is therefore another important open question.

Storage rings are an attractive source of electron beams for CBXFELs due to their high repetition rate and, in the fourth generation, low emittance. The favorable beam properties as well as the flexibility in operation mode makes SR XFELs with a cavity design a good candidate as future light source. Equipping storage ring light sources with XFELs would give more opportunities for conducting experiments needing high intensity coherent light pulses. Combining the feasibility of the CBXFEL concept with other technologies

such as the TGU would result in very bright coherent lasers in storage ring light sources. Due to the options for tunable optical cavities this would overall lead to more flexible storage ring light sources, without the need for construction of additional LINACs. Now that fourth generation facilities have been and are being constructed, along with the capability to produce highly reflective X-ray mirrors, the actual construction of CBXFELs is therefore a desirable next step.

6 References

[1] Nils Martensson and Mikael Eriksson. "The saga of MAX IV, the first multi-bend achromat synchrotron light source". In: *Nuclear Instruments and Methods in Physics Research Section A: Accelerators, Spectrometers, Detectors and Associated Equipment* 907 (2018). Advances in Instrumentation and Experimental Methods (Special Issue in Honour of Kai Siegbahn), pp. 97–104. ISSN: 0168-9002. DOI: https://doi.org/10.1016/j.nima.2018.03.018. URL: https://www.sciencedirect.com/science/article/pii/S016890021830353X.

[2] *Overview*. URL: https://www.xfel.eu/facility/overview/index_eng.html. (accessed: 08.02.2023).

[3] Stefan Günster et al. "Storage ring free-electron lasing at 176 nm-dielectric mirror development for vacuum ultraviolet free-electron lasers". In: *Applied optics* 45 (Sept. 2006), pp. 5866–70. DOI: 10.1364/AO.45.005866.

[4] Pedro Tavares et al. "Commissioning and first-year operational results of the MAX IV 3 GeV ring". In: *Journal of Synchrotron Radiation* 25 (Sept. 2018). DOI: 10.1107/S1600577518008111.

[5] Christian Schroer et al. "PETRA IV: the ultralow-emittance source project at DESY". In: *Journal of Synchrotron Radiation* 25 (Sept. 2018). DOI: 10.1107/S1600577518008858.

[6] Aliaksei Halavanau et al. "Experimental setup for high-resolution characterization of crystal optics for coherent X-ray beam applications". In: *Journal of Applied Crystallography* 56.1 (Feb. 2023), pp. 155–159. DOI: 10.1107/S1600576722010998. URL: https://doi.org/10.1107/S1600576722010998.

[7] Kwang-Je Kim and Yuri V. Shvyd'ko. "Tunable optical cavity for an x-ray free-electron-laser oscillator". In: *Phys. Rev. ST Accel. Beams* 12 (3 Mar. 2009), p. 030703. DOI: 10.1103/PhysRevSTAB.12.030703. URL: https://link.aps.org/doi/10.1103/PhysRevSTAB.12.030703.

[8] Z. Huang. "Brightness and coherence of synchrotron radiation and fels". In: (Jan. 2013), pp. 16–20.

[9] CONTRIWT. *Coherent Optics 101: Definition, Advantage, and More*. July 2022. URL: https://www.optcore.net/article062/. (accessed: 08.02.2023).

[10] Arthur L. Robinson. *X-Ray Data Booklet, Section 2.2 HISTORY of SYNCHROTRON RADIATION*. URL: https://xdb.lbl.gov/Section2/Sec_2-2.html. (accessed: 08.05.2023).

[11] R P Walker. "Synchrotron radiation". In: (1994). DOI: 10.5170/CERN-1994-001.437. URL: https://cds.cern.ch/record/398429.

[12] P Schmüser. "Free-electron lasers". In: (2006). DOI: 10.5170/CERN-2006-002.477. URL: http://cds.cern.ch/record/941330.

[13] Francesca Curbis. *Free Electron Lasers (FELs)*. URL: https://canvas.education.lu.se/courses/19277/files/2880105?module_item_id=699976. (accessed: 08.05.2023).

[14] Yuri Shvyd'ko. "Feasibility of X-Ray Cavities for Free Electron Laser Oscillators". In: *Beam Dynamics Newsletter* 60 (2013), pp. 68–83.

[15] Rachel Margraf et al. *Low-loss Stable Storage of X-ray Free Electron Laser Pulses in a 14 m Rectangular Bragg Cavity*. Jan. 2023. DOI: 10.21203/rs.3.rs-2465216/v1.

[16] Patrick Rauer et al. "Cavity based x-ray free electron laser demonstrator at the European X-ray Free Electron Laser facility". In: *Phys. Rev. Accel. Beams* 26 (2 Feb. 2023), p. 020701. DOI: 10.1103/PhysRevAccelBeams.26.020701. URL: https://link.aps.org/doi/10.1103/PhysRevAccelBeams.26.020701.

[17] Herman Winick. "Fourth generation light sources". In: (1998). URL: https://cds.cern.ch/record/336200.

[18] Christian G. Schroer and Hamburg DESY Dt. Elektr.-Synchr. *PETRA IV: upgrade of PETRA III to the Ultimate 3D X-ray microscope. Conceptual Design Report*. Ed. by Ralf Roehlsberger et al. Hamburg: Deutsches Elektronen-Synchrotron DESY, 2019, 259 pages : illustrations, diagrams. ISBN: 9783945931264. DOI: 10.3204/PUBDB-2019-03613. URL: https://bib-pubdb1.desy.de/record/426140.

[19] Ilya Agapov, Yong-Chul Chae, and Wolfgang Hillert. "Low Gain FEL Oscillator Option for PETRA IV". In: *9th International Particle Accelerator Conference*. June 2018. DOI: 10.18429/JACoW-IPAC2018-TUPMF069.

[20] Yuri Shvyd'ko and R. Lindberg. "Spatiotemporal Response of Crystals in X-ray Bragg Diffraction". In: *Physical Review Special Topics - Accelerators and Beams* 15 (July 2012). DOI: 10.1103/PhysRevSTAB.15.100702.

[21] Takashi Tanaka. "SIMPLEX: Simulator and postprocessor for free-electron laser experiments". In: *Journal of Synchrotron Radiation* 22 (Sept. 2015). DOI: 10.1107/S1600577515012850.

[22] A. Bernhard et al. "Transverse gradient undulator-based high-gain-FELs. A parameter study". In: *6th International Particle Accelerator Conference (IPAC 15), Richmond, Va., May 3-8, 2015 Proceedings publ.online Paper TUPWA039 JACoW, 2015*. 54.01.01; LK 01. 2015, pp. 1502–1505. ISBN: 978-3-95450-168-7.

[23] R. R. Lindberg and K.-J. Kim. "Mode growth and competition in the x-ray free-electron laser oscillator start-up from noise". In: *Phys. Rev. ST Accel. Beams* 12 (7 July 2009), p. 070702. DOI: 10.1103/PhysRevSTAB.12.070702. URL: https://link.aps.org/doi/10.1103/PhysRevSTAB.12.070702.

7 Appendix

Python code used for data analysis and plotting in Figures 5, 6, 7:

```
import numpy as np
import matplotlib.pyplot as plt

#%%  'Open Centered Spectrum'
file = 'K79285_noseed_bw4003'  # BW = 4.003
f = open(f'{file}', 'r')
data1 = np.genfromtxt(f)
np.delete(data1,0,0) # Erases the first row (i.e. the header)
f.close()
Energy_cntrd = data1[:,0]
Flux_cntrd = data1[:,1]

#%%  'Open detuned Spectrum'
file = 'Test_no_change_K793_noSeedPower'  # BW = 4.645
f = open(f'{file}', 'r')
data1 = np.genfromtxt(f)
np.delete(data1,0,0) # Erases the first row (i.e. the header)
f.close()
Energy = data1[:,0]
Flux = data1[:,1]

#%%  'Open SN'

file = 'SN_73'  # BW = 24.73
f = open(f'{file}', 'r')
data1 = np.genfromtxt(f)
np.delete(data1,0,0) # Erases the first row (i.e. the header)
f.close()
Energy_sn = data1[:,0]
Flux_sn = data1[:,1]

#%%  'Reflectivity / Bandwidth'

BW_min = 13005.1  # Diamond crystal bandwidth
BW_max = 13005.12
r = 0.99**3*0.95    # Reflectivity of cavity

R_cntrd = []        # List for reflectivity of cavity, K = 0.79285
R = []              # List for reflectivity of cavity, K = 0.793

Max_Flux, Max_Flux_R = [], []       # Lists for selection of max points
E_max_flux = []                     # Corresponding energy values
Max_Flux_cntrd, Max_Flux_cntrd_R = [], []
E_max_flux_cntrd = []
LL, LL_cntrd = [], []
```

```
LL2, LL2_cntrd = [], []

for i in range(len(Energy_cntrd)):  # Multiplying K=0.79285 with r
    if Energy_cntrd[i] >= BW_min and Energy_cntrd[i] <= BW_max:
        R_cntrd.append(Flux_cntrd[i]*r)
        if Energy_cntrd[i-1] != Energy_cntrd[i]:
            LL_cntrd.append(i)
        if Energy_cntrd[i+1] != Energy_cntrd[i]:
            LL_cntrd.append(i)
    else:
        R_cntrd.append(0)

for i in range(len(LL_cntrd)):
    if i%2 == 0:
        LL2_cntrd.append(LL_cntrd[i])
LL2_cntrd.append(LL_cntrd[-1])

for i in range(len(LL2_cntrd)-1):
    Max_Flux_cntrd.append(max(Flux_cntrd[LL2_cntrd[i]:LL2_cntrd[i+1]]))
    Max_Flux_cntrd_R.append(max(R_cntrd[LL2_cntrd[i]:LL2_cntrd[i+1]]))
    E_max_flux_cntrd.append(Energy_cntrd[LL2_cntrd[i]])


for i in range(len(Energy)):  # multiplying K=0.793 with r
    if Energy[i] >= BW_min and Energy[i] <= BW_max:
        R.append(Flux[i]*r)
        if Energy[i-1] != Energy[i]:
            LL.append(i)
        if Energy[i+1] != Energy[i]:
            LL.append(i)
    else:
        R.append(0)

for i in range(len(LL)):
    if i%2 == 0:
        LL2.append(LL[i])
LL2.append(LL[-1])

for i in range(len(LL2)-1):
    Max_Flux.append(max(Flux[LL2[i]:LL2[i+1]]))
    Max_Flux_R.append(max(R[LL2[i]:LL2[i+1]]))
    E_max_flux.append(Energy[LL2[i]])

#%%  'Undulator Cavity Comparison - centered'

plt.plot(Energy_cntrd, Flux_cntrd, marker = '.', linestyle = 'none',
    markersize = 5,
         label = 'Undulator radiation\nK=0.79285', color = 'darkorange')
```

```
plt.plot(Energy_cntrd, R_cntrd, marker = '.', linestyle = 'none', markersize = 5,
         label = 'Radiation after one\ncavity roundtrip', color = 'crimson')
plt.title('Total Photon Flux Spectrum\nComparison undulator and cavity')
plt.xlabel('Energy\n[eV]')
plt.ylabel('Flux\n[photons/pulse/0.1%/BW]')
plt.legend()
plt.grid()
plt.show()

#%%  'Undulator Cavity Comparison - detuned'

plt.plot(Energy, Flux, marker = '.', linestyle = 'none', markersize = 5,
         label = 'Undulator radiation, K=0.793', color = 'darkorange')
plt.plot(Energy, R, marker = '.', linestyle = 'none', markersize = 5,
         label = 'Radiation after one\ncavity roundtrip', color = 'crimson')
plt.title('Total Photon Flux Spectrum\nComparison undulator and cavity')
plt.xlabel('Energy\n[eV]')
plt.ylabel('Flux\n[photons/pulse/0.1%/BW]')
plt.legend()
plt.grid()
plt.show()

#%%  'SN comparison - no bw'

SN_max = max(Flux_sn[1:])
bw_spectrum = 4.645
bw_cntrd = 4.003
bw_sn = 24.73

spectrum = [bw_spectrum*0.001*Max_Flux_R[i] for i in range(len(Max_Flux_R))]
cntrd = [bw_cntrd*0.001*Max_Flux_cntrd_R[i] for i in range(len(Max_Flux_cntrd_R))]
sn = [bw_sn*0.001*SN_max for i in range(len(Energy_sn))]

plt.plot(E_max_flux_cntrd, cntrd, marker = 'o', linestyle = 'none',
         markersize = 7, label = 'Radiation after one\ncavity roundtrip,\nK=0.79285',
         color = 'crimson')
plt.plot(E_max_flux, spectrum, marker = 'D', linestyle = 'none',
         markersize = 7, label = 'Radiation after one\ncavity roundtrip,\nK=0.793',
         color = 'crimson')
plt.plot(Energy_sw, sn, label = 'maximum shot noise flux',
         linestyle = 'dotted', linewidth = 5, color = 'k')
```

```
plt.xlim(BW_min-0.005, BW_max + 0.005)
plt.xticks([BW_min, BW_max], [13005.10, 13005.12])
plt.title('Total Photon Flux Spectrum\nComparison cavity and shot noise\
    nwithin crystal bandwidth')
plt.xlabel('Energy\n[eV]')
plt.ylabel('Flux\n[photons/pulse]')
plt.legend(loc=(1.04, 0.3))
plt.grid()
plt.show()

#%%  'Calculating ratio flux spectrum : flux SN'

a = max(sn)/max(cntrd)
b = max(sn)/max(spectrum)

print(f'The ratio between the K = 0.79285 spectrum and SN is {a}')
print(f'So the cavity can accept up to {1-a} losses')
print('\n')
print(f'The ratio between the K = 0.793 spectrum and SN is {b}')
print(f'So the cavity can accept up to {1-b} losses')
```